Journal of Achievements in Materials and Manufacturing Engineering
VOLUME 38
ISSUE 2
February
2010

Springback prediction in V-die bending: modelling and experimentation

M.A. Osman [a], M. Shazly [b,*], A. El-Mokaddem [c], A.S. Wifi [c]
[a] Department of Industrial Engineering, Fayoum University, 63514 Egypt
[b] Department of Mechanical Engineering,
The British University in Egypt, 11837 Egypt
[c] Department of Mechanical Design and Production Engineering,
Faculty of Engineering, Cairo University, 12613 Egypt
* Corresponding author: E-mail address: mostafa.shazly@bue.edu.eg

Received 03.12.2009; published in revised form 01.02.2010

Analysis and modelling

ABSTRACT

Purpose: A theoretical model is developed for the air-bending process and V-die bending experiments are conducted. Based on comparisons between springback ratios predicted using the developed theoretical air bending model and the V-die bending experiments, a semi-empirical formula for predicting springback ratio in V-die bending process is suggested. The validity of this formula is verified using finite element simulations as well as comparisons with the results of two other independent sets of experiments.

Design/methodology/approach: A theoretical model for air bending is developed and compared with published models. Experimental work on V-die bending is conducted. The experimental results are used in a correlation analysis to develop a mathematical expression for predicting springback ratio of V-die bending as a correction of the spring back ratio of air bending. These results are verified by comparisons with finite element simulations as well as with other independent sets of experiments.

Findings: Springback ratios for V-die bending could be predicted using the developed semi-empirical formula. For a given limit of the striking (coining) force, springback ratios are affected by sheet thickness, bend radius, and material parameters.

Research limitations/implications: This work suggests a methodology for the prediction of springback ratio in V-die bending. This work can be extended by studying the effect of anisotropy on the developed springback ratio.

Practical implications: The developed semi-empirical formula could be practically used in determining the springback ratio for V-die bending. The selection of the sheet thickness and bend radius are critical parameters that affect springback ratios.

Originality/value: A semi-empirical formula is suggested for the prediction of springback ratio in V-die bending. This is viewed as a correction of the theoretically predicted air bending springback ratios. This formula could be of help to those working in sheet metal forming industries.

Keywords: Springback; V-die bending; Air bending; Finite element

Reference to this paper should be given in the following way:
M.A. Osman, M. Shazly, A. El-Mokaddem, A.S. Wifi, Springback prediction in V-die bending: modelling and experimentation, Journal of Achievements in Materials and Manufacturing Engineering 38/2 (2010) 179-186.

1. Introduction

Spring-back is a common phenomenon that occurs in sheet metal bending after unloading due to elastic recovery. It could be defined in terms of spring-back ratio K (the ratio between the produced and desired bend angles). Various efforts were made to analyse the spring-back phenomenon analytically, experimentally, and numerically for different shapes, and process and material parameters [1-8]. Most of the analytical studies focused on air bending while limited work was done on V-die bending due the inherent difficulties due to the coining action associated with this problem [9]. Previous studies [9-11] conducted on spring-back in V-bending showed that the material's grain size had little effect, while texture had relatively higher effect on spring-back. The spring-back was also found to be influenced by the bend radius and the process temperature with little effect of the punch speed. Finite element method was used to study the effect of different process parameters and validate analytical models in V-bending process by many workers e.g. [12, 13]. They showed that the spring-back was very much affected by punch radius, punch angle and die-lip radius.

In this study, a theoretical model for predicting spring-back ratio in air bending of an elastic-strain hardening material is developed. In contrast to the previously developed air bending models, the present analysis considers the true location of neutral fibre and logarithmic true strain instead of engineering strain. The spring back ratios obtained using this developed model is compared with previously developed models available in literature [1-3]. Furthermore, correlation analysis is used to develop a semi-empirical formula to express the experimentally measured spring-back ratio in V-die bending process. This formula is developed in terms of the theoretical air bending spring-back ratio, sheet thickness, bend radius and material parameters (n, C, and E). This formula is validated through comparisons with two independent sets of experimental results as well as finite element simulations.

2. Theoretical air bending model

The theoretical air bending models developed in the literature commonly adopt the simplifying assumptions detailed in Lange [14]; most notably that plane sections remain plane, mid fibre is the neutral fibre, and engineering plane strain condition is adopted. It seems interesting to assess if some of such simplifying assumptions could be relaxed. Here, the neutral fibre position is determined considering the continuity of the radial stresses [3]. Also the true logarithmic strain is adopted instead of the commonly adopted engineering strain.

Referring to Figure 1; applying the equilibrium condition it leads to [3]:

$$\frac{d\sigma_y}{dr} = \frac{\sigma_x - \sigma_y}{r} \tag{1}$$

The effective plastic strain and stress are given by [15]:

$$\bar{\varepsilon} = \frac{2}{\sqrt{3}}\left|\varepsilon_x\right| = \begin{cases} \dfrac{2}{\sqrt{3}}\ln\dfrac{r}{r_u} & ; r \geq r_u \\ \dfrac{2}{\sqrt{3}}\ln\dfrac{r_u}{r} & ; r \leq r_u \end{cases} \tag{2}$$

$$\bar{\sigma} = \begin{cases} +\dfrac{\sqrt{3}}{2}\left(\sigma_x - \sigma_y\right) & ; r \geq r_u \\ -\dfrac{\sqrt{3}}{2}\left(\sigma_x - \sigma_y\right) & ; r \leq r_u \end{cases} \tag{3}$$

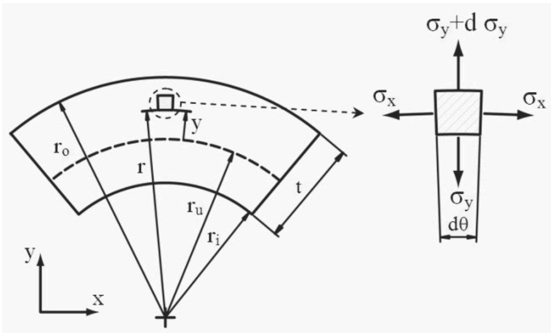

Fig. 1. Equilibrium of forces

Substituting Equation (3) into (1) yields:

$$\frac{d\sigma_y}{dr} = \begin{cases} +\dfrac{2}{\sqrt{3}}\dfrac{\bar{\sigma}}{r} & ; r \geq r_u \\ -\dfrac{2}{\sqrt{3}}\dfrac{\bar{\sigma}}{r} & ; r \leq r_u \end{cases} \tag{4}$$

For a strain hardening behaviour following Hollomon's formula, $\bar{\sigma} = C\bar{\varepsilon}^n$, it can be shown that

$$\sigma_y = \frac{C'}{n+1}\begin{cases} \ln^{n+1}\dfrac{r}{r_u} - \ln^{n+1}\dfrac{r_o}{r_u} & ; r \geq r_u \\ \ln^{n+1}\dfrac{r_u}{r} - \ln^{n+1}\dfrac{r_u}{r_i} & ; r \leq r_u \end{cases} \tag{5}$$

where r_u is the neutral fibre given by [3]:

$$r_u = \sqrt{r_i r_o} \tag{6}$$

The circumferential true stress is given by

$$\sigma_y = C'\begin{cases} \left(\ln^n\dfrac{r}{r_u} + \dfrac{1}{n+1}\left(\ln^{n+1}\dfrac{r}{r_u} - \ln^{n+1}\dfrac{r_o}{r_u}\right)\right) & ; r \geq r_u \\ \left(-\ln^n\dfrac{r_u}{r} + \dfrac{1}{n+1}\left(\ln^{n+1}\dfrac{r_u}{r} - \ln^{n+1}\dfrac{r_u}{r_i}\right)\right) & ; r \leq r_u \end{cases} \tag{7}$$

Referring to Figure 1; $y = r - r_u$, thus $dy = dr$ (8)

Assuming small elastic core, then the total bending moment is given by [16]:

$$M = M_{el} + M_{pl} \cong M_{pl} = \int_{y=r_i-r_u}^{y=0} \sigma_x b y dy + \int_{y=0}^{y=r_o-r_u} \sigma_x b y dy \tag{9}$$

Substituting Equation (7) into (9) and integrating yields:

$$\therefore M = C'b \left(\begin{array}{c} -\int_{r_i}^{r_u} r \ln^n \frac{r_u}{r} dr + r_u \int_{r_i}^{r_u} \ln^n \frac{r_u}{r} dr \\ + \frac{1}{n+1} \int_{r_i}^{r_u} r \ln^{n+1} \frac{r_u}{r} dr - \frac{r_u}{n+1} \int_{r_i}^{r_u} \ln^{n+1} \frac{r_u}{r} dr \\ + \int_{r_i}^{r_o} r \ln^n \frac{r}{r_u} dr - r_u \int_{r_u}^{r_o} \ln^n \frac{r}{r_u} dr \\ + \frac{1}{n+1} \int_{r_u}^{r_o} r \ln^{n+1} \frac{r}{r_u} dr - \frac{r_u}{n+1} \int_{r_u}^{r_o} \ln^{n+1} \frac{r}{r_u} dr \\ + \left(\begin{array}{c} \frac{(r_u - r_i)^2}{2(n+1)} \ln^{n+1} \frac{r_u}{r_i} \\ - \frac{(r_o - r_u)^2}{2(n+1)} \ln^{n+1} \frac{r_o}{r_u} \end{array} \right) \end{array} \right) \tag{10}$$

Successive integrations by parts for Equation (10) yields:

$$M = \delta \left(\begin{array}{c} -\beta^{-2} \sum_{i=1}^{\infty} \frac{(-1)^{i-1}(-2)^{i-1} \ln^{i-1}\beta}{\prod_{j=1}^{i}(n+j)} \\ + \beta^{-1} \sum_{i=1}^{\infty} \frac{(-1)^{i-1}(-1)^{i-1} \ln^{i-1}\beta}{\prod_{j=1}^{i}(n+j)} \\ + \frac{\beta^{-2}}{n+2} \ln\beta \sum_{i=1}^{\infty} \frac{(-1)^{i-1}(-2)^{i-1} \ln^{i-1}\beta}{\prod_{j=1}^{i}(n+1+j)} \\ - \frac{\beta^{-1}}{n+2} \ln\beta \sum_{i=1}^{\infty} \frac{(-1)^{i-1}(-1)^{i-1} \ln^{i-1}\beta}{\prod_{j=1}^{i}(n+1+j)} \\ + \beta^{2} \sum_{i=1}^{\infty} \frac{(-1)^{i-1} 2^{i-1} \ln^{i-1}\beta}{\prod_{j=1}^{i}(n+j)} - \beta \sum_{i=1}^{\infty} \frac{(-1)^{i-1} \ln^{i-1}\beta}{\prod_{j=1}^{i}(n+j)} \\ + \frac{\beta^{2}}{n+2} \ln\beta \sum_{i=1}^{\infty} \frac{(-1)^{i-1} 2^{i-1} \ln^{i-1}\beta}{\prod_{j=1}^{i}(n+1+j)} \\ - \frac{\beta}{n+2} \ln\beta \sum_{i=1}^{\infty} \frac{(-1)^{i-1} \ln^{i-1}\beta}{\prod_{j=1}^{i}(n+1+j)} \\ + \frac{1}{2(n+1)} \left[\left(1 - \frac{1}{\beta}\right)^2 - (\beta - 1)^2 \right] \end{array} \right) \tag{11}$$

where $\delta = C' b r_u^2 \ln^{n+1} \beta; \quad \beta = r_u / r_i = r_o / r_u$

Equation (11) is numerically evaluated using MATLAB by considering a finite number of terms for each expansion so that the change in the total bending moment obtained is less than 10^{-6}.

Since unloading is elastic [2], change in circumferential stress for $r_i \le r \le r_o$ is:

$$\Delta\sigma_x = E' \Delta\varepsilon_x = E' \left(\ln \frac{r}{r_u} - \ln \frac{r}{r'_u} \right) \tag{12}$$

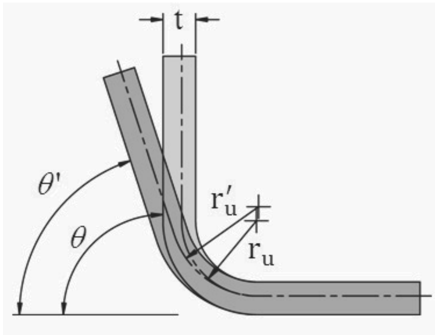

Fig. 2. Spring-back phenomenon

Referring to Figure 2, the spring-back ratio K is given by:

$$K = \frac{\theta'}{\theta} = \frac{r_u}{r'_u} \tag{13}$$

Substituting from Equations (8) and (13) into (12) yields:

$$\Delta\sigma_x = E' \left(\ln\left(\frac{y}{r_u} + 1 \right) - \ln\left(\frac{Ky}{r_u} + 1 \right) \right) \tag{14}$$

Using Equation (14), the change in moment is:

$$\Delta M = \int_{r_i - r_u}^{r_o - r_i} \Delta\sigma_x b y dy = E' b r_u^2 \left(P_1 + P_2 + \frac{P_3}{K^2} + \frac{P_4}{K^2} \right) \tag{15}$$

where:

$$P_1 = \frac{1}{2} \left(\beta^2 \left[\ln\beta - \frac{1}{2} \right] - \left(\frac{1}{\beta} \right)^2 \left[\ln \frac{1}{\beta} - \frac{1}{2} \right] \right);$$

$$P_2 = -\beta[\ln\beta - 1] + \frac{1}{\beta}\left[\ln\frac{1}{\beta} - 1 \right];$$

$$P_3 = -\frac{1}{2}\begin{pmatrix} \left(\left(K[\beta-1]+1\right)^2 \left[\ln\left(K[\beta-1]+1\right) - \frac{1}{2} \right] \right) \\ -\left(\left(K\left[\frac{1}{\beta}-1\right]+1 \right)^2 \left[\ln\left(K\left[\frac{1}{\beta}-1\right]+1 \right) - \frac{1}{2} \right] \right) \end{pmatrix};$$

$$P_4 = \begin{pmatrix} \left(\left(K[\beta-1]+1\right)\left[\ln\left(K[\beta-1]+1\right)-1\right] \right) \\ -\left(\left(K\left[\frac{1}{\beta}-1\right]+1 \right) \left[\ln\left(K\left[\frac{1}{\beta}-1\right]+1 \right) - 1 \right] \right) \end{pmatrix}.$$

In view of Equations (11) and (15) and since $M\text{-}\Delta M = 0$ after spring-back; the highly nonlinear equation $M\text{-}\Delta M = f\ (K) = 0$ is numerically solved using MATLAB to obtain the exact value of K_{Air}.

3. Experimental work

3.1. Material

V-die bending experiments are conducted on 38 mm x100 mm annealed steel specimens cut from 1000 mm x 2000 mm commercially available cold rolled low carbon steel sheets having thicknesses of 0.7, 1.5, and 2.5 mm. The specimens are cut in such a way that their length directions are normal to the rolling direction for better bendability. Two other sets of specimens are cut from as received commercially available cold rolled low carbon steel sheets and as received commercially available aluminium sheets. These sets will be used for the validation of the V-die bending spring-back formula presented in Section 5. The mechanical properties obtained from uniaxial tension tests are given in Table 1.

Table 1.
Mechanical properties of work materials

As Received Steel						
t (mm)	E (GPa)	v	σ_Y (MPa)	σ_{ult} (MPa)	C (MPa)	n
0.7	207.69	0.3033	335.32	503.27	653.72	0.1594
1.5	207.91	0.3038	306.15	495.88	636.84	0.1597
2.5	207.83	0.3035	300.45	438.18	551.54	0.1405
Annealed Steel						
t (mm)	E (GPa)	v	σ_Y (MPa)	σ_{ult} (MPa)	C (MPa)	n
0.7	207.14	0.3005	290.58	467.49	664.34	0.2499
1.5	207.12	0.3011	288.97	466.83	666.85	0.2480
2.5	207.10	0.3002	276.86	459.06	663.74	0.2441
As-received commercially pure Aluminium						
t (mm)	E* (GPa)	v*	σ_Y (MPa)	σ_{ult} (MPa)	C (MPa)	n
0.7	70	0.27	92.18	152.2	236.9	0.108
1.5	70	0.27	66.25	127.9	375.1	0.253
2.5	70	0.27	60.10	104.0	144.6	0.083

* Ref. [14]

3.2. V-bending experiments

A semi closed 90° V-die is designed and used to conduct bending process. The die assembly consists of a die having a 1 mm die valley radius, and a punch having four inserts with different nose radii of 1, 3, 5, and 8 mm. The die assembly is installed on the compression side of a 100 KN universal testing machine (WDW-100D). The V-die bending processes are conducted under constant coining force of 100 kN.

For experimental measuring the spring-back, a digital PC camera is fixed on the die assembly and connected to a laptop as shown in Figure 3. The camera is adjusted so that it is normal to the V-die opening. The spring-back produced is measured by taking two images for the fully loaded and unloaded bent specimens [17]. The images are then imported into a drafting software in which two straight lines are drawn on the V-profile of both the upper and lower sheet surfaces and bend angles θ and θ' shown in Figure 2 are measured.

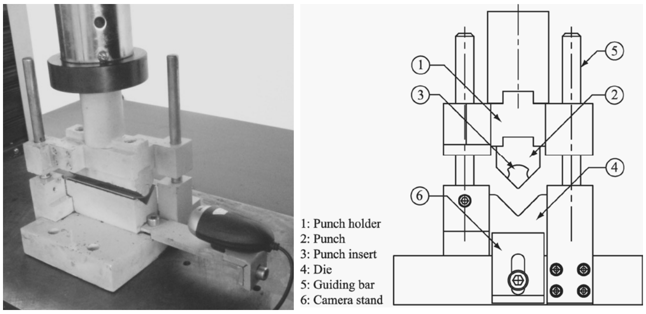

Fig. 3. The experimental setup for the V-die bending

Three experiments are conducted for each sheet thickness-bend radius combination. The loaded and unloaded bend angles are measured three times on each of the upper and lower sheet surfaces for each experiment and then averaged. The resultant spring-back ratio for each sheet thickness-bend radius is then obtained by averaging the values of the spring-back ratios for the three experiments.

4. Finite Element Modelling

Finite element simulations for V-die bending were carried out using ABAQUS/Explicit and ABAQUS/Standard modules. The loading stage was simulated using ABAQUS/Explicit module while the unloading stage and spring-back calculations were carried out using ABAQUS/Standard [17]. Due to process symmetry, only one half of the tools and workpiece are modelled. Punch and die were modelled as analytical rigid parts and plane strain condition was assumed. The material model used was as isotropic linear elastic-work hardening material with properties determined as per the tensile experiments. The friction coefficient between the sheet and the tooling surfaces was initially adjusted in such a way that the load and displacement obtained from the finite element simulations agreed with those obtained experimentally.

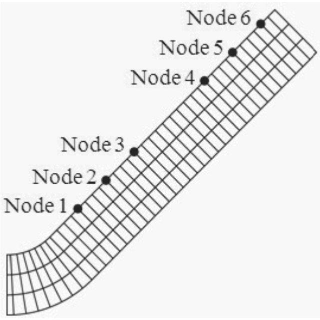

Fig. 4. Spring-back calculation

The amount of spring-back was determined using the coordinates of six nodes distributed along the inner sheet surface [17] as shown in Figure 4. The slopes of straight lines connecting the node pairs (1, 4), (2, 5), and (3, 6) were obtained and averaged to calculate spring-back ratio $K_{Num.}$.

5. Results and discussions

Figure 5 shows comparisons between spring-back ratios predicted using the developed theoretical air bending model K_{Air} and spring-back ratios predicted using other published theoretical air bending models [1-3]. As shown in Figure 5, the spring-back ratios predicted using various approaches do have general agreement despite of the seemingly different assumptions made in analyses.

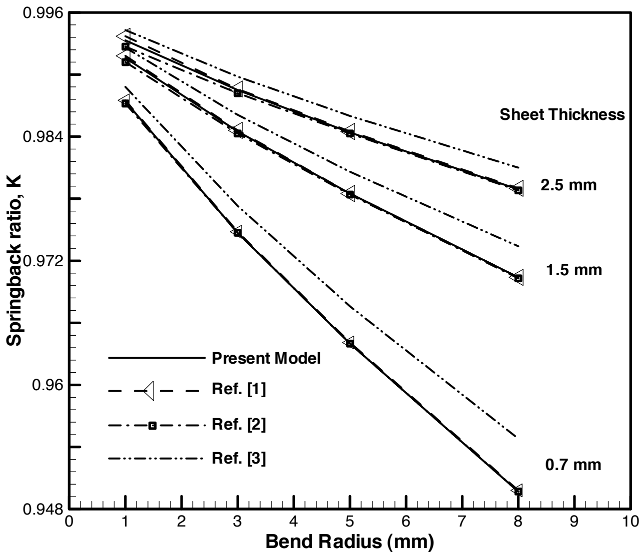

Fig. 5. Present theoretical spring-back ratio in comparison to other published models for annealed steel

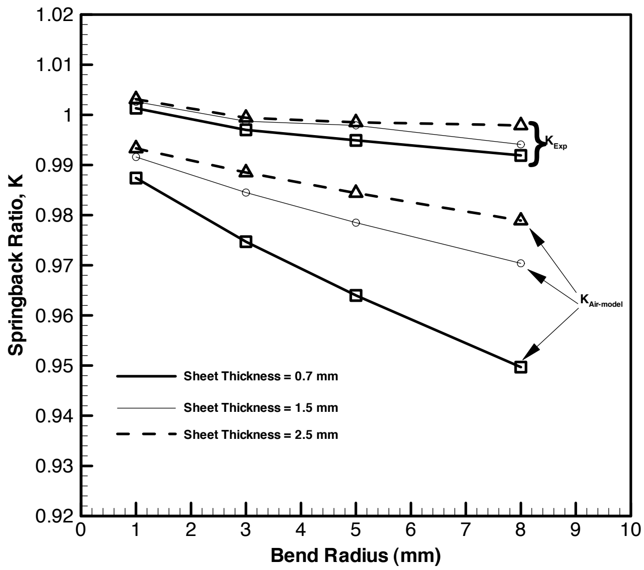

Fig. 6. Present theoretical spring-back ratio for air bending (K_{Air}) and experimental V-die spring-back ratios (K_{Exp}) for annealed steel

The effect of the coining stage in V- die bending process on increasing the spring-back ratio as compared to air bending is shown in Figure 6. For a specific sheet thickness t, increasing the bend radius r_p decreases the spring-back ratio in V-die bending. It is worth noting that negative spring-back ratios (K >1) are frequently obtained when bending to the smallest bend radius (as reflected with r_p=1 mm). Generally, for a specific bend radius r_p, increasing the sheet thickness the spring-back ratio in V-die bending is increased. This means that increasing the sheet thickness, the bend angles quality is enhanced reducing the spring-back generated.

5.1. A formula for Springback ratio in V-die bending

Based on Figure 6 and using correlation analysis, a semi-empirical formula is developed to determine the spring-back ratio in V-die bending process. The material and process parameters are selected similarly to those used by Yuen [18] where a_1, a_2, a_3 and a_4 are fit constants determined using the built in curve fitting schemes in MATLAB. The spring-back ratio in V-die bending K_{V-die}, Equation (16), is expressed as a correction of the theoretical air bending spring-back ratio K_{Air}.

$$K_{V-die} = K_{Air}\left[a_1 + a_2\left(\frac{C'}{E'}\right)\left(\frac{a_3 t}{r_u}\right)^{n-a_4}\right] \quad (16)$$

For the present analysis, with a coining force of 100 kN, the constants produced by MATLAB are a_1 = 1.0045, a_2 = 1.12,

a_3 = 1.0, and a_4 = 1.02 respectively. To determine the validity of the developed equation for predicting spring-back ratio in V-die bending $K_{V\text{-}die}$, the predicted values are tested over a wide range of material's parameters (E, C, and n) and compared against finite element simulations. Moreover, the two independent sets of experimental results for the as-received steel and aluminium are compared with those obtained using the developed Equation (16). Figures 7 to 9 show V-die spring-back ratio from Equation (16) and finite element simulations are in good agreement. In these figures, lines represent Equation (16) while symbols represent results of the finite element simulations.

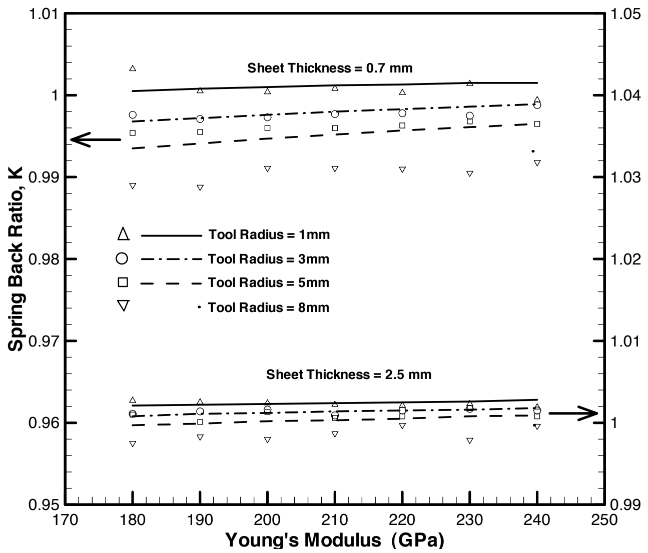

Fig. 7. Effect of Young's modulus "E" on spring-back ratio

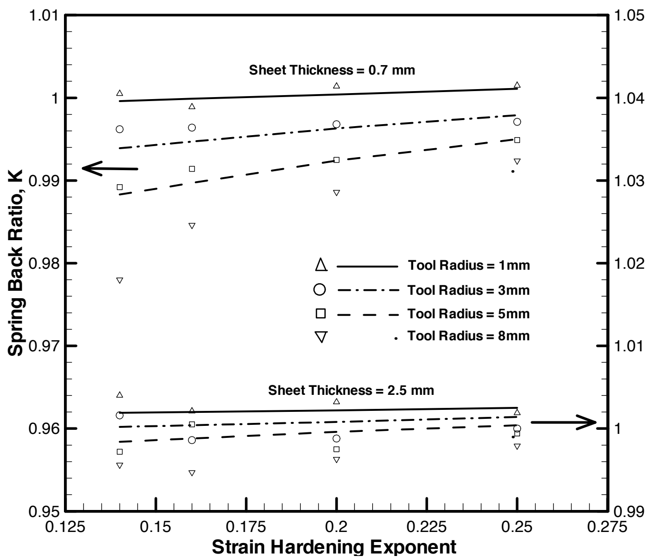

Fig. 8. Effect of Strain Hardening Exponent "n" on spring-back

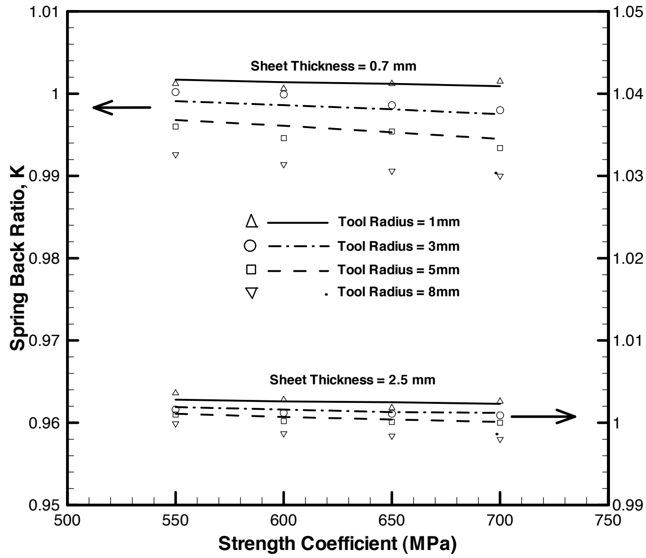

Fig. 9. Effect of Strength Coefficient "C" on spring-back ratio

Figures 10 and 11 show comparisons between experimental results for V-die bending conducted on as-received steel and as-received aluminium. As shown in these figures, Equation (16) agrees well with experimental results for these two independent sets of experiments. The results depicted in Figures 6 to 10 suggest that the developed formula is validated for different materials and thicknesses with a coining force of 100 kN and in the range of the present working conditions. Similar formulas could be developed for other working conditions following similar methodology.

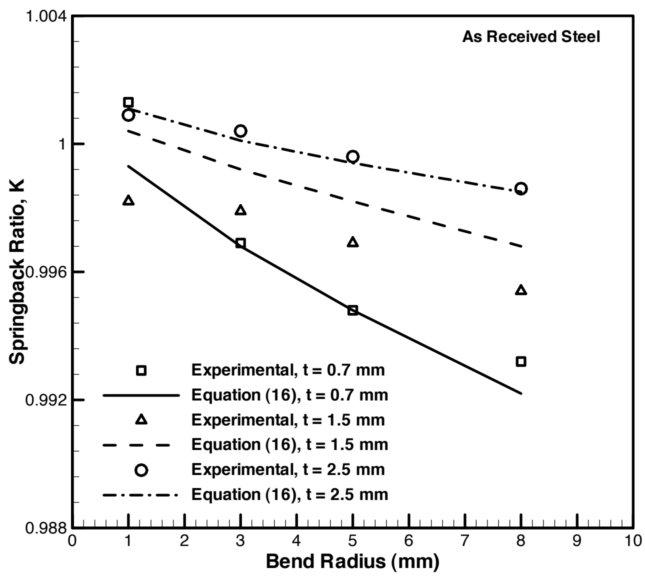

Fig. 10. Comparison between spring-back ratio obtained experimentally and using Equation (16) for as-received steel

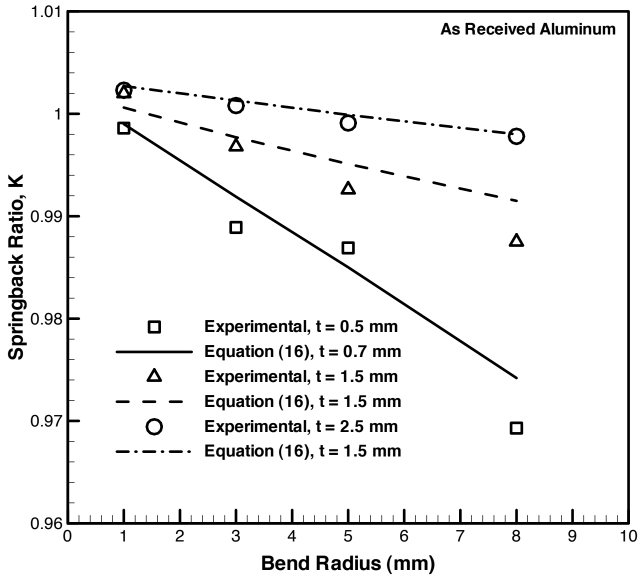

Fig. 11. Comparison between spring-back ratio obtained experimentally and using Equation (16) for as-received aluminium

6. Conclusions

A theoretical model for air bending has been developed using true strain and neutral fibre position that satisfy continuity of the radial stress. This was found to compare it well with the published models. Experimental work on V-die bending of annealed steel has been conducted on specially designed die. The experimental results have been used in a correlation analysis to develop a semi-empirical formula for predicting spring-back ratio in V-die bending process, $K_{V\text{-}die}$, as a correction of the theoretical spring back ratio of air bending, K_{air}. The results of this formula have been verified, for a given coining force and working conditions, by the agreement about comparisons with finite element simulations as well as about other independent sets of experiments made on as-received steel and as-received aluminium of various thicknesses.

Nomenclature

b, t	Sheet width and thickness
C'	Plane strain Strength coefficient; $C' = C\left(2/\sqrt{3}\right)^{n+1}$
E'	Plane strain Young's modulus; $E'=E/(1-\nu^2)$
K	Spring-back ratio; $K=\theta'/\theta$
M	Total bending moment
M_{el}, M_{pl}	Elastic and Plastic portions of the bending moment
n	Strain hardening exponent
r	Radius of curvature at distance "y" from neutral plane
r_i, r_o	Radii of curvatures at the inner and outer surfaces
r_m	Radius of curvature for the middle plane under loading
r_m'	Radius of curvature for the middle plane after unloading
r_p	Radius of punch insert (bend radius)
r_u	Radius of curvature for the neutral plane under loading
r_u'	Radius of curvature for the neutral plane after unloading
y	Distance from neutral plane
ΔM	Change in bending moment due to elastic unloading
ε_x	Circumferential true strain
$\bar{\varepsilon}$	Effective strain
θ, θ'	The bend angle under loading and after unloading
υ	Poisson's ratio
σ_{ult}	Uniaxial ultimate strength
σ_x	Circumferential true stress
σ_y	Radial true stress
σ_Y	Uniaxial yield stress
$\bar{\sigma}$	Effective stress
μ	Coefficient of friction

References

[1] C.A. Queener, R.J. De Angelis, Elastic spring-back and residual stresses in sheet metal formed by bending, Transactions of ASME 61 (1968) 757-768.

[2] W.F. Hosford, R.M. Caddell, Metal Forming: Mechanics and Metallurgy, Prentice-Hall, Englewood Cliffs, New Jork, 1983.

[3] D.-K. Leu, A Simplified Approach for Evaluating Bendability and Spring-back in Plastic Bending of Anisotropic Sheet Metals, Journal of Materials Processing Technology 66 (1997) 9-17.

[4] Z. Marciniak, J.L. Duncan, S.J. Hu, Mechanics of Sheet Metal Forming, Second Edition, Butterworth-Heinemann Press, 2002.

[5] T. Da Sisva Botelho, E. Bayraktar, G. Inglebert, Comparison of Experimental and Simulation Results of 2D-draw-bend Spring-back, Journal of Achievements in Materials and Manufacturing Engineering 18 (2006) 275-278.

[6] F.-K. Chen, S.-F. Ko, Deformation Analysis of Spring-back in L-bending of Sheet Metal, Journal of Achievements in Materials and Manufacturing Engineering 18 (2006) 339-342.

[7] A. Gnatowski, P. Palutkiewicz, E. Bociąga, Numerical Analysis of Stress State During Single Point Bending in DMTA Examinations, Journal of Achievements in Materials and Manufacturing Engineering 28/1 (2008) 47-50.

[8] T. Ohashi, H. Chiba, H. Takano, Employment of Concentrated-Hard Sphere-Suspension Pad for V-bending of Thin Strip, Journal of Achievements in Materials and Manufacturing Engineering 31/2 (2008) 699-704.

[9] D-K Leu, C-M Hsieh, The Influence of Coining Force on Spring-Back Reduction in V-Die Bending Process, Journal of Materials Processing Technology 196 (2008) 230-235.

[10] Z. Tekiner, An Experimental Study on the Examination of Spring-back of Sheet Metals with Several Thicknesses and Properties in Bending Dies, Journal of Materials Processing Technology 145 (2004) 109-117.

[11] Ö. Tekaslan, U. Şeker, A. Özdemir, Determining Spring-back Amount of Steel Sheet Metal Has 0.5 mm Thickness in

Bending Dies, Journal of Materials and Design 27 (2006) 251-258.
[12] A. Nilsson, L. Melin, C. Magnusson, Finite-Element Simulation of V-Die Bending: A Comparison with Experimental Results, Journal of Materials Processing Technology 65 (1997) 52-58.
[13] W.M. Chan, H.I. Chew, H.P. Lee, B.T. Cheok, Finite Element Analysis of Spring-back of V-Bending Sheet Metal Forming Processes, Journal of Materials Processing Technology 148 (2004) 15-24.
[14] K. Lange, Handbook of metal forming, McGraw-Hill Company, 1985.
[15] P. Dadras, S.A. Majlessi, Plastic Bending of Work Hardening Materials, Journal of Engineering for Industry 104 (1982) 224-230.
[16] L.J. de Vin, A.H. Streppel, U.P. Singh, H.J.J. Kals, A process Model for Air Bending, Journal of Materials Processing Technology 57 (1996) 48-54.
[17] J.A. Ferreira, P. Sun, J.J. Gracio, Closed Loop Control of a Hydraulic Press for Spring-back Analysis, Journal of Materials Processing Technology 177 (2006) 377-381.
[18] W.Y.D. Yuen, A Generalized Solution for the Prediction of Spring-back in Laminated Strip, Journal of Materials Processing Technology 61 (1996) 254-264.